JOURNAL OF SYNCHROTRON RADIATION

ISSN 1600-5775

Received 16 June 2015
Accepted 23 September 2015

Edited by S. M. Heald, Argonne National Laboratory, USA

Keywords: EXAFS; americium; coordination chemistry; lactate; aqueous speciation.

An EXAFS spectroscopic study of Am(III) complexation with lactate

Daniel R. Fröhlich,[a]* Andrej Skerencak-Frech,[b] Ugras Kaplan,[b] Carsten Koke,[a,b] André Rossberg[c] and Petra J. Panak[a,b]

[a]Physikalisch-Chemisches Institut, Ruprecht-Karls-Universität Heidelberg, Im Neuenheimer Feld 253, Heidelberg 69120, Germany, [b]Institut für Nukleare Entsorgung, Karlsruher Institut für Technologie, PO Box 3640, Karlsruhe 76021, Germany, and [c]Institut für Resourcenökologie, Helmholtz-Zentrum Dresden-Rossendorf, PO 510119, Dresden 01314, Germany. *Correspondence e-mail: daniel.froehlich@partner.kit.edu

The pH dependence (1–7) of Am(III) complexation with lactate in aqueous solution is studied using extended X-ray absorption fine-structure (EXAFS) spectroscopy. Structural data (coordination numbers, Am—O and Am—C distances) of the formed Am(III)–lactate species are determined from the raw k^3-weighted Am L_{III}-edge EXAFS spectra. Between pH 1 and pH 6, Am(III) speciation shifts continuously towards complexed species with increasing pH. At higher pH, the amount of complexed species decreases due to formation of hydroxo species. The coordination numbers and distances (3.41–3.43 Å) of the coordinating carbon atoms clearly point out that lactate is bound 'side-on' to Am(III) through both the carboxylic and the α-hydroxy function of lactate. The experimentally determined coordination numbers are compared with speciation calculations on the basis of tabulated thermodynamic stability constants. Both EXAFS data and thermodynamic modelling are in very good agreement. The EXAFS spectra are also analyzed by iterative transformation factor analysis to further verify the determined Am(III) speciation and the used structural model.

1. Introduction

The final disposal of high-level nuclear waste will be performed in deep geological formations. Besides rock salt and crystalline formations (*e.g.* granite), clay rocks are taken into account as potential host rock formations in several European countries [*e.g.* Belgium (ONDRAF/NIRAS, 2001), France (OECD, 2006), Germany (Hoth *et al.*, 2007), Switzerland (NAGRA, 2002)]. Due to their long half-lives, the transuranium elements (Np, Pu, Am) will determine the long-term radiotoxicity of the nuclear waste material. As reducing conditions are expected in the near-field of the repository (Bradbury & Baeyens, 2003), +III will be the stable oxidation state of Pu and Am. Thus, the trivalent actinides are of particular interest for a reliable long-term safety assessment.

In case of a release of radionuclides from their primary containments during the storage time, a detailed knowledge of the relevant interaction mechanisms of these contaminants with the surrounding host rock, backfill material and aquifer is essential. The relevant interaction processes include complexation reactions with inorganic and organic ligands present in the pore waters of natural clays. Courdouan *et al.* (2007*a*,*b*) characterized the dissolved organic compounds in the pore waters of different natural clays (*i.e.* Callovo Oxfordian and Opalinus Clay) and showed that low-molecular-weight compounds (formate, acetate, propionate, lactate, *etc.*) make up large fractions of the dissolved organic matter.

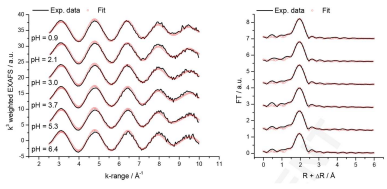

Table 1
Composition of the samples.

Sample	pH	[Am(III)] (mol L^{-1})	[Lactate] (mol L^{-1})
1	0.9	2.7×10^{-4}	8.5×10^{-3}
2	2.1	1.6×10^{-4}	5.0×10^{-3}
3	3.0	1.5×10^{-4}	4.6×10^{-3}
4	3.7	1.3×10^{-4}	3.9×10^{-3}
5	5.3	1.4×10^{-4}	4.3×10^{-3}
6	6.4	1.4×10^{-4}	4.4×10^{-3}

The present study is focused on the complexation of Am(III) with lactate in aqueous solution at varying pH-value.

Among the low-molecular-weight compounds, lactate is particularly interesting as it offers different possible coordination modes in contrast to simple carboxylic ligands (*e.g.* acetate, propionate). Lactate can either coordinate 'end-on' through the carboxylic function only or 'side-on' through both the carboxylic and the α-hydroxy group. Furthermore, the coordination mode might change with varying pH-value. In this study, the molecular structure of Am(III)–lactate species (coordination numbers and interatomic distances) is studied systematically between pH 1 and pH 7 using extended X-ray absorption fine-structure (EXAFS) spectroscopy. This pH range is chosen to exclude the formation of Am(III) hydroxo and carbonate species which are formed at pH $\geq$ 7, thus enabling the exclusive investigation of Am(III) lactate species.

The interaction of Am(III) with lactate has been the topic of several thermodynamic studies determining stability constants for the formation of different Am(III)–lactate complexes (Aziz & Lyle, 1971; Barkleit *et al.*, 2014; Lundqvist *et al.*, 1984; Sakanoue & Nakatani, 1972; Zalupski *et al.*, 2010). However, no EXAFS data of complexes between lactate and Am(III) or other trivalent actinides are found in the literature. Even for actinides of other oxidation states, structural data are scarce. There is only one publication, by Lucks (2012), investigating the complexation of U(VI) with lactate. Thus, the present work will provide structural data for the complexation of Am(III) with lactate for the first time and, thus, will add to a molecular-level understanding of actinide geochemistry. Furthermore, Am(III) data can also be used to describe the geochemical behavior of Pu(III).

2. Experimental section

2.1. Sample preparation

Six samples were prepared from an Am(III) stock solution containing 6.9×10^{-3} *M* ^{243}Am and 2.2×10^{-4} *M* ^{241}Am and a lactate stock solution containing 3.7×10^{-2} *M* sodium lactate (Sigma-Aldrich). The pH values of the samples were adjusted using diluted solutions of HCl (Merck, Suprapure) or NaOH (Merck, Titrisol). The concentration of Am(III) was measured by γ-spectrometry. pH measurements were carried out using a combination pH electrode (Ross, ORION), which was calibrated with standard buffer solutions (Merck, Titrisol, pH 3, 6, 10). Details on the composition and pH of the samples are given in Table 1. 200 µL of each sample solution were encapsulated in PE vials and sealed in PE foil before transporting to the synchrotron facility.

Table 2
Standard state stability constants of the different complexation reactions used for speciation calculations.

All constants were obtained from the NIST databases 46.6, 46.7, 46.8 and from Plummer & Busenberg (1982).

Reaction	Log K^0
$Am^{3+} + H_2O \rightleftharpoons AmOH^{2+} + H^+$	−6.497
$Am^{3+} + 2H_2O \rightleftharpoons Am(OH)_2^+ + 2H^+$	−14.094
$Am^{3+} + 3H_2O \rightleftharpoons Am(OH)_3$ (aq) + $3H^+$	−25.691
$Am^{3+} + CO_3^{2-} \rightleftharpoons AmCO_3^+$	7.8
$Am^{3+} + 2CO_3^{2-} \rightleftharpoons Am(CO_3)_2^-$	12.3
$Am^{3+} + Lac^- \rightleftharpoons AmLac^{2+}$	3.04
$Am^{3+} + 2Lac^- \rightleftharpoons AmLac_2^+$	5.22
$Am^{3+} + 3Lac^- \rightleftharpoons AmLac_3$ (aq)	7.32
$H^+ + Lac^- \rightleftharpoons HLac$ (aq)	3.86
$Na^+ + H_2O \rightleftharpoons NaOH$ (aq) + H^+	−13.897
$H_2O \rightleftharpoons H^+ + OH^-$	−13.997
$H^+ + CO_3^{2-} \rightleftharpoons HCO_3^-$	10.329
$2H^+ + CO_3^{2-} \rightleftharpoons H_2CO_3$ (aq)	16.681
$Na^+ + H^+ + CO_3^{2-} \rightleftharpoons NaHCO_3$ (aq)	10.029
$Na^+ + CO_3^{2-} \rightleftharpoons NaCO_3^-$	1.27

2.2. EXAFS spectroscopy

Am L_{III}-edge EXAFS spectra of the samples were obtained in fluorescence mode using a 13-element Ge-detector at the Rossendorf Beamline (ROBL, BM20) at the European Synchrotron Radiation Facility (ESRF, Grenoble, France). The detector was positioned at an angle of 90° relative to the incoming beam. For energy calibration, a zirconium foil was measured simultaneously in transmission mode. Details on the design and the equipment of the beamline are given elsewhere (Matz *et al.*, 1999). Data processing, including energy calibration, averaging, extraction of the EXAFS signal and fitting, was performed using the software package *EXAFSPAK* (George & Pickering, 2000). In all cases the ionization energy of Am (E_0) was set to 18515 eV. Theoretical scattering phases and amplitudes were calculated with *FEFF8.20* (Ankudinov *et al.*, 2002) using the crystal structure of [YbL^1Lactate](CF$_3$SO$_3$)$_2$ (Dickins *et al.*, 2002; L^1 is a heptadentate ligand) in which lactate is bound 'side-on' to Yb as model crystal structure (Yb replaced by Am). The potentials were calculated using the self-consistent field approach. In every case the best theoretical model was fit to the raw k^3-weighted EXAFS spectra using the Marquardt algorithm. The amplitude reduction factor S_0^2 was held constant at 0.9.

2.3. Speciation calculations

The Am(III) speciation under experimental conditions (compare Table 1) has been calculated using the software package *Visual MINTEQ* (version 3.0) (Gustafsson, 2012). Ionic strength corrections are taken into account using the Davies equation (Davies, 1938). The thermodynamic stability constants of the complexation reactions considered in the calculations are given in Table 2. The stability constants were

obtained from the NIST databases 46.6, 46.7, 46.8 and from Plummer & Busenberg (1982).

2.4. ITFA

The EXAFS spectra were analyzed by iterative transformation factor analysis (ITFA; Rossberg *et al.*, 2003). A detailed description of the application of ITFA to the complexation of actinides with organic ligands and the different analysis steps during this procedure are given elsewhere (Lucks *et al.*, 2012). In the present work, ITFA is used to evaluate the experimental EXAFS spectra by applying two components, *i.e.* Am(III) with a complete water shell and a hypothetical Am(III) species completely coordinated by ligands. In the latter case, all oxygen atoms in the first coordination sphere belong to coordinating functional groups of lactate. The resulting component spectra are extracted and fitted with *EXAFSPAK* following the same procedure as for the experimental spectra.

3. Results

3.1. Speciation calculations

Before evaluation of the experimental data, the Am(III) speciation has been calculated for each sample with *Visual MinteQ* (version 3.0). The results are presented in Table 3. Up to pH = 2, the speciation is almost quantitatively determined by the Am(III) aquo ion. With increasing pH, the speciation shifts visibly towards complexed species. Above pH 3.7, $AmLac^{2+}$ is the dominating species; above pH 5, $AmLac_2^+$ makes up more than 20% of the total Am(III) speciation. $AmLac_3$ (aq) is present at about 10% at pH > 5. Only at pH = 6.4 are minor amounts of hydoxo and carbonato species present.

Table 3
Speciation of Am(III) calculated with *Visual MINTEQ* (version 3.0) for the experimental conditions given in Table 1 using the thermodynamic constants given in Table 2.

Amounts of species are given in % (species < 1% not shown).

Sample	pH	Am^{3+}	$AmLac^{2+}$	$AmLac_2^+$	$AmLac_3$ (aq)	$AmOH^{2+}$	$AmCO_3^+$
1	0.9	100	–	–	–	–	–
2	2.1	95	5	–	–	–	–
3	3.0	66	32	2	–	–	–
4	3.7	38	50	10	2	–	–
5	5.3	17	50	23	10	1	–
6	6.4	15	45	21	10	8	1

3.2. EXAFS

The raw k^3-weighted Am L_{III}-edge EXAFS spectra of samples 1–6 together with the corresponding Fourier transforms (FTs) and the fit curves are shown in Fig. 1. In the case of samples 1 and 2, no visible contribution of lactate is expected (compare Table 3). The spectra of samples 3–6 have either been fitted with or without the shells of the coordinating carbon and the distal carbon/oxygen neighbors. The resulting fit parameters are given in Table 4. During the fitting procedure, the Debye–Waller factors (σ) of the second and third coordination sphere were held constant at 0.005 $Å^2$. The coordination number (N) of the distal C/O atoms has been linked to the coordination number of the coordinating carbon. In all cases the reduced error decreases when taking the carbon shells into account, thus confirming the presence of lactate in the coordination sphere of Am(III). For all samples, 10–11 oxygen atoms at a radial distance (R) of 2.47 Å are found in the first coordination sphere. These values are in good agreement with reported data for Am(III) and other trivalent actinides in aqueous solution (Allen *et al.*, 2000; Brendebach *et al.*, 2009; Fröhlich *et al.*, 2015). Between pH 3.0 and 5.3, the coordination number with respect to carbon increases continuously from 1.0 and 2.2, whereas at higher pH the coordination number decreases due to the formation of hydroxo species as expected from the thermodynamic calcu-

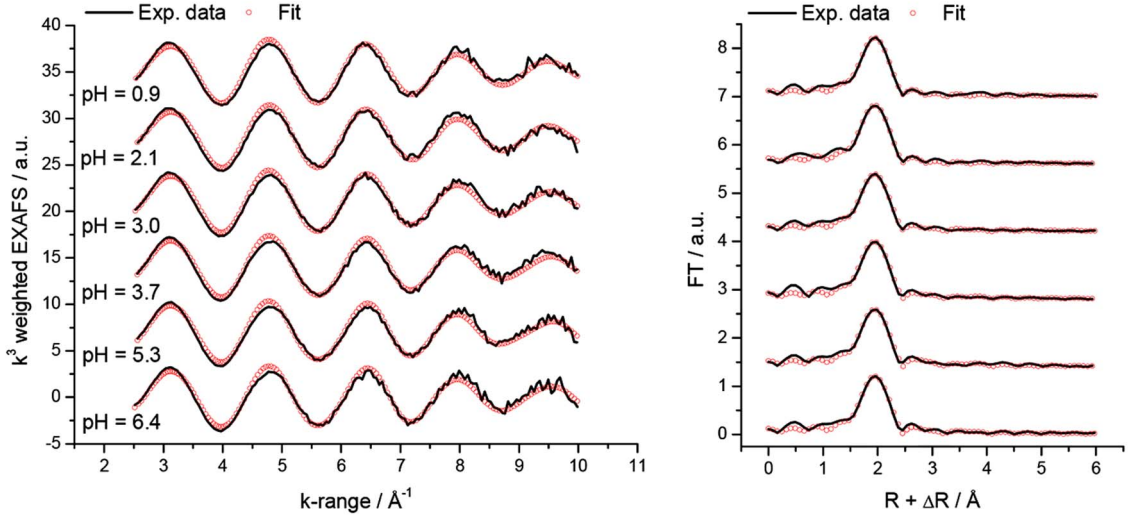

Figure 1
Left: raw k^3-weighted Am L_{III}-edge EXAFS spectra (black dots) of Am(III) in the presence of lactate as a function of the pH (detailed experimental conditions are given in Table 1) together with the best fit from *EXAFSPAK* (red lines). Right: corresponding Fourier transforms (FTs).

lations (compare §3.1). The coordinating carbon neighbors are located at 3.41–3.43 Å, the distal C/O neighbors at 4.32–4.36 Å. The distance of the coordinating carbon is significantly larger than those determined for Am(III)–acetate complexes. In the latter case, R(Am—C) ranges between 2.78 and 2.84 Å (Fröhlich *et al.*, 2015). This discrepancy clearly points out the differences regarding the coordination mode of these two ligands. As a result, lactate binds 'side-on' to Am(III) in contrast to acetate, which coordinates 'end-on' through the carboxylic function only. Barkleit *et al.* (2014) investigated the 1:1 complex of Eu(III), which is frequently used as a surrogate for trivalent actinides, with lactate by ^{1}H- and ^{13}C-NMR, also showing that Eu(III) is coordinated by the carboxylic and the hydroxy group. Furthermore, it was shown that the hydroxy group seems to become deprotonated when the complex with Eu(III) is formed. The Am—C distances are comparable with the U(VI) data of Lucks (2012) with the U—C distance for the UO_2Lac^+ and the UO_2Lac_2 (aq) species equal to 3.52 ± 0.02 Å. This value is slightly larger compared with the present finding which is attributed to structural differences as U(VI) forms UO_2^{2+} cations.

From our results it can be concluded that Am(III) is coordinated by lactate in a 'side-on' fashion through the carboxylic and the α-hydroxy functional group forming a chelate complex. For the chosen experimental conditions, no change of the coordination mode with increasing pH, reflected by a change in the Am—C distance, is observed.

The experimental results are compared with the results of the thermodynamic speciation calculations given in Table 3. Using these data, the average coordination number with respect to lactate has been calculated for each sample. A comparison of the calculated coordination numbers and the EXAFS data is shown in Table 5. Assuming 'side-on' coordination of lactate over the whole experimental range, the number of coordinating ligands equals $N(C_{coord}) \times 0.5$. As can be seen from Table 5, the predictions of the thermodynamic calculations and the experimental results are in very good agreement which again confirms the binding-mode of lactate being 'side-on'.

Table 4
Fit parameters of the raw k^3-weighted Am L_{III}-edge EXAFS spectra shown in Fig. 1.

Sample		1	2	3	4	5	6
pH		0.9	2.1	3.0	3.7	5.3	6.4
O	N	10.9 (3)	10.4 (3)	10.6 (3)	10.4 (4)	10.2 (3)	10.0 (4)
	R (Å)	2.47 (1)	2.47 (1)	2.47 (1)	2.47 (1)	2.47 (1)	2.47 (1)
	σ^2 (Å^2)	0.0104 (4)	0.0099 (4)	0.0103 (4)	0.0103 (4)	0.0100 (5)	0.0094 (5)
C_{coord}†	N	–	–	1.0 (4)	1.6 (4)	2.2 (4)	1.7 (5)
	R (Å)	–	–	3.43 (4)	3.43 (3)	3.41 (2)	3.42 (2)
C/O_{distal}‡	R (Å)	–	–	4.34 (5)	4.36 (4)	4.36 (3)	4.32 (4)
ΔE_0 (eV)		−1.7 (3)	−1.5 (3)	−1.4 (2)	−1.4 (3)	−1.4 (3)	−1.3 (3)
Reduced error without C shells		0.1357	0.1460	0.1282	0.1678	0.1671	0.1978
Reduced error with C shells		–	–	0.1266	0.1578	0.1430	0.1843
k-range (Å^{-1})		2.54–9.99	2.56–9.98	2.53–9.99	2.56–9.98	2.56–9.98	2.52–9.99

† Debye–Waller factor (σ^2) held constant at 0.005 Å^2. ‡ The coordination number (N) of C/O_{distal} is linked to N of C_{coord}. σ^2 is held constant at 0.005 Å^2. The amplitude reduction factor (S_0^2) is set to 0.9 in all cases. The uncertainties of each value obtained from the *EXAFSPAK* fit are given in parentheses. The absolute errors in N and the radial distances (R) are: N ± 20%, R ± 0.02 Å (Li *et al.*, 1995).

Table 5
Comparison of the average number of ligands coordinated to Am(III) obtained by EXAFS spectroscopy and thermodynamic speciation calculation.

	Average number of ligands obtained from†	
Sample	EXAFS	Speciation calculation
1	0	0
2	0	0.1
3	0.5 ± 0.2	0.4
4	0.8 ± 0.2	0.8
5	1.1 ± 0.2	1.3
6	0.9 ± 0.3	1.2

† Assuming 'side-on' coordination of lactate.

3.3. ITFA

The raw Am L_{III}-edge EXAFS spectra are analyzed by ITFA. As stated above, the spectra are evaluated using two species, the Am(III) aquo ion and a hypothetical Am(III) species completely coordinated by lactate. The pure component EXAFS spectra are analyzed with *EXAFSPAK* following the same procedure as for the experimental data. The EXAFS spectra of components 1 and 2 together with the FTs and fit curves are shown in Fig. 2. In the FT of component 2, the contributions of the coordinating carbon and distal carbon/oxygen neighbors are clearly visible. It is also obvious that the EXAFS spectrum of component 2 exhibits a significantly lower signal-to-noise ratio than the spectrum of component 1 or the experimental EXAFS spectra (see Fig. 1), which is due to the low amount of component 2 throughout the series of spectra (maximum: 21%). The obtained fractions of the two components obtained from ITFA are shown in Table 6. As in the EXAFS experiment, the coordination number increases continuously up to pH 5.3 and then slightly decreases at higher pH. The resulting fit parameters are given in Table 7. Component 1 has 10.8 oxygen neighbors at 2.47 Å which is in excellent agreement with the findings for EXAFS samples 1 and 2. Due to the large noise in the case of component 2, a shorter k-range had to be chosen and the fitting has been carried out without consideration of the distal C/O neighbors. For component 2, the coordination number and distance with respect to oxygen are slightly lower [N(O) = 9.2, Am—O = 2.44 Å]. The coordination number of the coordinating carbon equals 9.5 which agrees with the coordination number of oxygen within the error range. Assuming 'side-on' coordination, the coordination numbers for oxygen in the first coordination sphere and the coordinating carbon neighbors are expected to be equal, which again verifies the used structural model. The coordinating carbon

Table 6
Fractions of the two components of the EXAFS pH-series determined by ITFA.

		Amount of component (%)	
Sample	pH	Component 1	Component 2
1	0.9	100	0
2	2.1	100	0
3	3.0	91	9
4	3.7	85	15
5	5.3	79	21
6	6.4	83	17

Table 7
Fit parameters of the k^3-weighted EXAFS spectra of components 1 and 2 obtained from ITFA (Fig. 2).

Component		1	2
O	N	10.8 (3)	9.2 (1.1)
	R (Å)	2.47 (1)	2.44 (1)
	σ^2 (Å^2)	0.0104 (4)	0.0108 (18)
C_{coord}†	N	–	9.5 (1.4)
	R (Å)	–	3.38 (1)
ΔE_0		−1.4 (2)	−2.9 (7)
Reduced error		0.1166	1.0749
k-range		2.03–9.99	2.03–8.62

† σ^2 is held constant at 0.005 Å^2. S_0^2 was set to 0.9. Uncertainties of each value obtained from the *EXAFSPAK* fit are given in parentheses. The absolute errors are: $N \pm 20\%$, $R \pm 0.02$ Å (Li *et al.*, 1995).

neighbors are located at 3.38 Å. This value agrees with the findings for the experimental EXAFS spectra within the error range.

4. Summary

Structural data of Am(III)–lactate species in the pH range 1–7 have been determined from Am L_{III}-edge EXAFS measurements. For all samples, 10–11 oxygen neighbors at 2.47 Å are found in the first coordination sphere. Between pH 3.0 and 5.2, the coordination number with respect to carbon increases from 1.0 to 2.2. Further increase of pH results in a decrease of N(C) to 1.7 due to formation of hydroxo species. The coordinating carbon and the distal carbon/oxygen neighbors are located at 3.41–3.43 and 4.32–4.36 Å, respectively. The obtained distances clearly point out that lactate binds in a 'side-on' fashion to Am(III) through both the carboxylic and the α-hydroxy function of the ligand, thus forming a chelate complex. The EXAFS data are compared with predictions based on thermodynamic speciation calculations. Both the thermodynamic model and the experimental results are in very good agreement.

The experimental EXAFS spectra have been evaluated with two components using ITFA. Component 1, representing the Am(III) aquo ion, yields 10.8 oxygen neighbors at 2.47 Å. The fit of the EXAFS spectrum of component 2 which should correspond to Am(III) completely coordinated with ligands shows 9.2 oxygen atoms in the first coordination sphere at a distance of 2.44 Å. The coordination number of carbon (9.5 ± 1.4) agrees with the number of O atoms within the error range, confirming the structural model. The coordinating carbon neighbors are located at 3.38 ± 0.01 Å which agrees very well with the experimental data.

This work clearly shows that the systematic investigation of small organic compounds, being potential ligands for actinides in nuclear waste repository scenarios, by EXAFS spectroscopy yields important structural information and enables the distinction of different coordination modes (*e.g.* 'end-on', 'side-on'). The presently determined structural data are a valuable contribution to safety analysis of nuclear waste disposal and will help to improve the molecular-level understanding of complexation reactions of actinides in aqueous solution. Furthermore, data obtained for Am(III) can also be used to predict the geochemical properties of Pu(III).

Acknowledgements

This work has been supported by the German Federal Ministry for Economic Affairs and Energy (BMWi) under

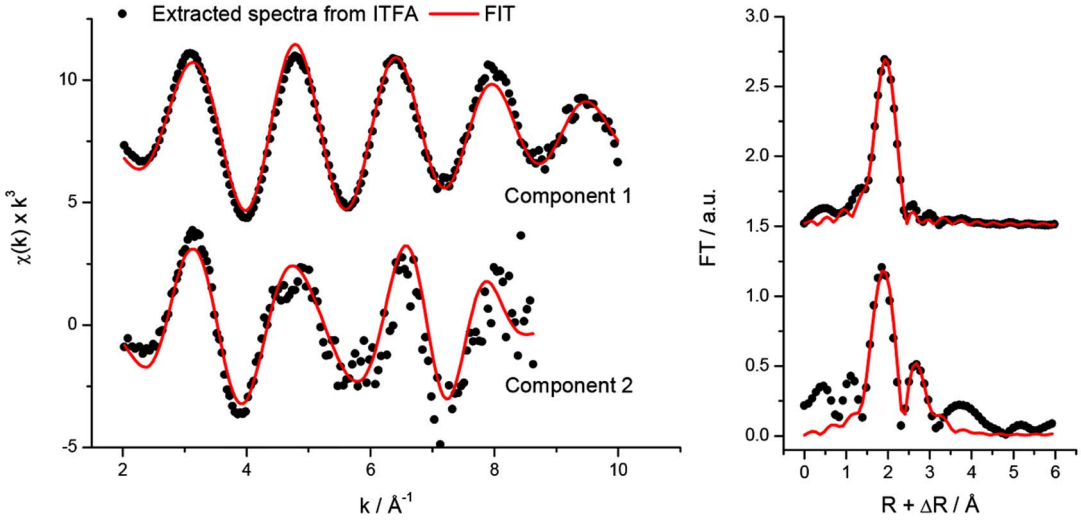

Figure 2
Left: k^3-weighted EXAFS spectra of components 1 and 2 obtained from ITFA. Right: corresponding Fourier transforms (FTs).

contract No. 02E11031 and the TALISMAN (Transnational Access to Large Infrastructure for a Safe Management of Actinide) program. All EXAFS measurements have been performed at the Rossendorf Beamline (ROBL, BM20) at the European Synchrotron Radiation Facility (ESRF, Grenoble, France). The authors thank C. Hennig, R. Butzbach and A. C. Scheinost for their assistance during our measurements. M. Fuss is acknowledged for performing the γ-measurements of the EXAFS samples.

References

Allen, P. G., Bucher, J. J., Shuh, D. K., Edelstein, N. M. & Craig, I. (2000). *Inorg. Chem.* **39**, 595–601.

Ankudinov, A. L., Bouldin, C. E., Rehr, J. J., Sims, J. & Hung, H. (2002). *Phys. Rev. B*, **65**, 104107.

Aziz, A. & Lyle, S. J. (1971). *J. Inorg. Nucl. Chem.* **33**, 3407–3408.

Barkleit, A., Kretzschmar, J., Tsushima, S. & Acker, M. (2014). *Dalton Trans.* **43**, 11221–11232.

Bradbury, M. H. & Baeyens, B. (2003). *Far field sorption data bases for performance assessment of a high-level radioactive waste repository in an undisturbed Opalinus Clay host rock.* PSI Technical Report 03–08. Paul Scherrer Institut, Villigen, Switzerland.

Brendebach, B., Banik, N. L., Marquardt, C. M., Rothe, J., Denecke, M. A. & Geckeis, H. (2009). *Radiochim. Acta*, **97**, 701–708.

Courdouan, A., Christl, I., Meylan, S., Wersin, P. & Kretzschmar, R. (2007*a*). *Appl. Geochem.* **22**, 1537–1548.

Courdouan, A., Christl, I., Meylan, S., Wersin, P. & Kretzschmar, R. (2007*b*). *Appl. Geochem.* **22**, 2926–2939.

Davies, C. W. (1938). *J. Chem. Soc.* pp. 2093–2098.

Fröhlich, D. R., Skerencak-Frech, A., Bauer, N., Rossberg, A. & Panak, P. J. (2015). *J. Synchrotron Rad.* **22**, 99–104.

George, G. N. & Pickering, I. J. (2000). *EXAFSPAK: A suite of computer programs for analysis of X-ray absorption spectra.* Stanford Synchrotron Radiation Laboratory, Stanford, USA.

Gustafsson, J. P. (2012). *Geochemical equilibrium speciation model Visual MINTEQ (version 3.0)*. KTH Royal Institute of Technology, Department of Land and Water Resources Engineering, Stockholm, Sweden.

Hoth, P., Wirth, H., Reinhold, K., Bräuer, V., Krull, P. & Feldrappe, H. (2007). *Endlagerung radioaktiver Abfälle in tiefen geologischen Formationen Deutschlands – Untersuchung und Bewertung von Tongesteinsformationen.* BGR Bundesanstalt für Geowissenschaften und Rohstoffe, Hannover, Germany.

Li, G. G., Bridges, F. & Booth, C. H. (1995). *Phys. Rev. B*, **52**, 6332–6348.

Lucks, C. (2012). PhD thesis, Institut für Ressourcenökologie, Helmholtz-Zentrum Dresden-Rossendorf, Dresden, Germany.

Lucks, C., Rossberg, A., Tsushima, S., Foerstendorf, H., Scheinost, A. C. & Bernhard, G. (2012). *Inorg. Chem.* **51**, 12288–12300.

Lundqvist, R., Lu, J.-F., Svantesson, I., Maeda, M. & Ohtaki, H. (1984). *Acta Chem. Scand.* **38*a***, 501–512.

Matz, W., Schell, N., Bernhard, G., Prokert, F., Reich, T., Claußner, J., Oehme, W., Schlenk, R., Dienel, S., Funke, H., Eichhorn, F., Betzl, M., Pröhl, D., Strauch, U., Hüttig, G., Krug, H., Neumann, W., Brendler, V., Reichel, P., Denecke, M. A. & Nitsche, H. (1999). *J. Synchrotron Rad.* **6**, 1076–1085.

NAGRA (2002). *Projekt Opalinuston – Synthese der geowissenschaftlichen Untersuchungsergebnisse, Entsorgungsnachweis für abgebrannte Brennelemente, verglaste hochaktive sowie langlebige mittelaktive Abfälle.* Technical Report NTB 02–03. NAGRA Nationale Genossenschaft für die Lagerung radioaktiver Abfälle, Wettingen, Switzerland.

OECD (2006). *Safety of geological disposal of high-level and long-lived radioactive waste in France – An international peer review of the 'Dossier 2005 Argile' concerning disposal in the Callovo-Oxfordian formation.* NEA No. 6178. OECD Organisation for Economic Co-operation and Development.

ONDRAF/NIRAS (2001). *SAFIR 2: Safety assessment and feasibility interim report.* NIROND-2001–06 E. ONDRAF/NIRAS, Brussels, Belgium.

Plummer, L. N. & Busenberg, E. (1982). *Geochim. Cosmochim. Acta*, **46**, 1011–1040.

Rossberg, A., Reich, T. & Bernhard, G. (2003). *Anal. Bioanal. Chem.* **376**, 631–638.

Sakanoue, M. & Nakatani, M. (1972). *Bull. Chem. Soc. Jpn*, **45**, 3429–3433.

Zalupski, P. R., Nash, K. I. & Martin, L. R. (2010). *J. Solution Chem.* **39**, 1213–1229.